ORIGINAL ARTICLE

Liquiritigenin Decreases Aβ Levels and Ameliorates Cognitive Decline by Regulating Microglia M1/M2 Transformation in AD Mice

Yexiang Du[1,2] · Min Luo[1] · Yehong Du[3] · Mingliang Xu[1] · Qiuhui Yao[1] · Kejian Wang[1] · Guiqiong He[1]

Abstract

Alzheimer's disease (AD) is one of the most common neurodegenerative diseases and is currently incurable. Amyloid β protein (Aβ) deposition is the main pathogenesis of AD, and many studies have shown that Aβ accumulation is toxic to neurons, leading to the inflammatory reaction, neuronal apoptosis, and neurofibrillary tangles. Thus, reducing Aβ levels might be a potential therapeutic strategy for AD. Liquiritigenin (LG), a dihydroflavone monomer compound extracted from natural plant licorice, has a variety of biological activities such as antioxidant, anti-tumor, anti-inflammatory and anti-virus. However, the exact function of LG in the pathogenesis of AD is elusive. Here, we reported that LG could significantly attenuate neuronal apoptosis in Aβ-induced N2A cells and APP/PS1 transgenic mice. Our in vivo and in vitro studies revealed that LG could alleviate the inflammation response, reflected by the reduction of NLRP3 and cleaved caspase-1. Meanwhile, we also found that LG was able to shift M1 type microglia towards M2 type microglia in Aβ-induced BV2 cells and AD mice. Furthermore, LG could reduce the Aβ levels by decreasing APP processing and accelerating Aβ clearance in AD mice. More importantly, daily treatment of LG (30 mg/kg day) for 90 days dramatically ameliorated the spatial learning and memory of AD mice. Taken together, these results suggest that LG can reduce the Aβ levels by regulating the M1/M2 transformation of microglia, thereby reversing memory decline during AD development, suggesting that LG may be a potential therapeutic agent for treating AD.

Keywords Alzheimer's disease · Liquiritigenin · Neuroinflammation · Cognition · Amyloid β protein · Microglia

✉ Guiqiong He
  guiqionghe@cqmu.edu.cn

1 Department of Anatomy, Basic Medical College, Chongqing Medical University, 1 Yixueyuan Road, Yuzhong District, Chongqing 400016, People's Republic of China

2 Department of Gastroenterology, Xinqiao Hospital, Army Medical University, Chongqing 400037, China

3 Pediatric Research Institute, Ministry of Education Key Laboratory of Child Development and Disorders, National Clinical Research Center for Child Health and Disorders, China International Science and Technology Cooperation Base of Child Development and Critical Disorders, Chongqing Key Laboratory of Translational Medical Research in Cognitive Development and Learning and Memory Disorders, Children's Hospital of Chongqing Medical University, Chongqing 400014, China

Introduction

Alzheimer's disease (AD) is a neurodegenerative disease characterized by the accumulation of amyloid β protein (Aβ) formed extracellular plaques (2019). Growing evidence shows that Aβ plays a culprit role in the pathogenesis of AD and has become the main therapeutic target (Bohm et al. 2015; Nakamura et al. 2018; Qiang et al. 2017; Takasugi et al. 2003). Aβ is generated from abnormal proteolytic cleavage of amyloid precursor protein (APP) by β-secretase (BACE1) and γ-secretase. The BACE1 cleaves APP at two β-sites to generate C99 and C89 fragments, respectively. Subsequently, C99 is cleaved by γ-secretase to produce Aβ, whereas it is normally cleaved by α- and γ-secretases (Tan and Gleeson, 2019). In addition to increasing generation, a reduction in Aβ clearance is essential for Aβ aggregation (Jang et al. 2018), while insulin-degrading enzyme (IDE) and neprilysin (NEP), produced in microglia cells, have the ability to degrade Aβ (Kong et al. 2010).

It is now well accepted that microglia, innate immune cells in the central nervous system, play a pivotal role in the onset and development of AD (Gogoleva et al. 2019; Hurtley, 2017). The chronic activation of NLRP3 inflammasome in microglia is the key and basic process of microglia-mediated neuroinflammation (Garcez et al. 2019; Liu et al. 2018). NLRP3 alters Aβ pathology by negatively regulating microglia clearance capacity, while the mice that have knocked out the NLRP3 can improve the clearance of Aβ (Chan et al. 2019; Fan et al. 2017). Activated microglia are classified into M1 and M2 types (Sierra-Filardi et al. 2011). M1 types including IL-1β, TNF-α, IL-6, IL-12, and IL-18 have the ability to promote the inflammatory response, while the M2 types, such as IL-4, IL-10, and IL-13, are to engulf cell debris and suppress immune inflammation (Ji et al. 2018; Yousefi et al. 2019).

Liquiritigenin (LG), a dihydroflavone monomer compound extracted from natural plant licorice, has a variety of biological activities such as antioxidant, anti-inflammatory, anti-tumor, and anti-virus (Ramalingam et al. 2018; Zhu et al. 2018). Recent study has shown that LG can ameliorate the inflammation response and memory decline in the Aβ-induced AD model mice (Hongyan et al. 2016; Jo et al. 2016a; Liu et al. 2009). However, the progress of AD is difficult to be mimicked by exogenous Aβ treatment, and so far, little is known about the pathogenesis of LG in AD development. In the current study, APP/PS1 transgenic AD model mice were selected and used to investigate the effect of LG on AD pathological changes and cognitive functions.

Materials and Methods

Animals

Three-month-old female APP/PS1 double transgenic mice (Nanjing, China) were used. APPSwe is the Swedish mutation of the amyloid precursor protein, and PS1 is the mutant form of human presenilin 1 (Theriault et al. 2016). AD mice were randomly assigned to LG (Must Bio-Technology, Chengdu) treatment group ($n = 10$) (30 mg/kg), and vehicle control ($n = 10$) was used as control. The LG-treated group received liquiritigenin continuously for 90 days (i.g.) before behavior assessment; the WT and vehicle-treated AD mice were treated with an identical volume (20 ml/kg) of vehicle (0.1% sodium carboxymethyl cellulose). The treatment has not been stopped during behavioral training.

Cell Culture and Treatment

Mouse neuroblastoma cell line N2A cells and microglial cell line BV2 were purchased from ATCC and cultured in 10% FBS and 90% Dulbecco's modified Eagle's medium (DMEM). The cell is maintained at 37 °C in 5% CO_2 atmosphere.

Cell Viability Assay

Cells were plated into 96-well plates (1×10^4 cells per well) in the presence of the Aβ (0, 2.5, 5, 10, 20, 50, and 100 μM) and LG (0, 2.5, 5, 10, 20, 50, and 100 μM) at the increasing doses. After 24 h, MTT (5 mg/ml) assay was used to measure cell viability. DMSO (200 μl) was added to each well to dissolve the purple formazan crystals. The absorbance was measured using a microplate reader at a wavelength of 490 nm (Bio-Rad, USA).

Quantitative Real-time PCR

Trizol reagent (TaKaRa, Japan) was used to extract total RNA from the cells, and the brain tissues of AD mice and spectrophotometer NanoDrop 2000 (Nanodrop Technologies, USA) were used to detect the purity of RNA. One microgram of RNA was used to performed synthesis of the first-strand complementary DNA (cDNA) with Prime Script RT reagent Kit with gDNA Eraser (TaKaRa, Japan) reverse transcriptase (TaKaRa, Japan). SYBR® Premix Ex Taq™ II (TaKaRa, Japan) was used to perform quantitative real-time PCR analysis with CFX (Bio-Rad). The primers are as follows:

IL-1β (forward: 5′-AGGCTCCGAGATGAACAA-3′, reverse: 5′-AAGGCATTAGAAACAGTCC-3′), TNF-α (forward: 5′-CTTCTCATTCCTGCTTGTG-3′, reverse: 5′-ACTTGGTGGTTTGCTACG-3′), IL-4 (forward: 5′-AACA GCCTCACAGAGCAGAAGAC-3′, reverse: 5′-GCCC TGCAGAAGGTTTCCTT-3′), IL-13 (forward: 5′-AGCA TGGTATGGAGTGTGGACCTG-3′, reverse: 5′-CAGT TGCTTTGTGTAGCTGAGCAG-3′), and β-actin (forward: 5′-GCACCACACCTTCTACAATGAGC-3′, reverse: 5′-GGATAGCAGCCTGGATAGCAAC-3′).

Immunohistochemical Staining

The immunohistochemical staining procedure was performed as previously published (Katoh et al. 1995). After sacrificing the mice, half of the brains were fixed in 4% paraformaldehyde and sectioned into 30 μm thickness. Every twelfth slice with the same reference position was mounted onto slides for staining. The monoclonal 4G8 antibody was used to detect the senile plaques.

Western Blot Assay

After treatment, cells were washed with pre-cold PBS, then lysed in RIPA lysis buffer (Beyotime, China) containing a cocktail of complete protease inhibitors (Roche), and centrifuged (4 °C, 12,000 rpm, 15 min) to collect the cell

supernatant. According to the instructions, the protein concentration was determined using BCA method (Beyotime, China). Thirty micrograms of protein sample was obtained and boiled in 5× loading buffer at 100 °C for 10 min, then electrophoresed with SDS-PAGE gel, and transferred to immobilon-PTM polyvinylidene fluoride (PVDF) membrane. Place the membrane in 5% skim milk in Tris-buffered saline containing 0.1% Tween-20 (TBST) at 37 °C for 1 h. Incubated with antibodies, NLRP3 (1:1000, Abcam, USA), caspase-1 (1:1000, Abcam, USA), caspase-3 (1:1000, CST, USA), cleaved-caspase-3 (1:1000, CST, USA), iNOS (1:500, Affinity, USA), Arg-1 (1:500, Affinity, USA), PS1(1:1000, Abcam, USA), APP (1:1000, Abcam, USA), and BACE1 (1:1000, CST, USA), CTF was obtained from UBC (1:1000) at 4 °C overnight and rinsed thrice with TBST for 5 min. β-actin (1:3000, CST, USA) was the internal reference. The band intensity of each protein was quantified by the Bio-Rad Quantity One software.

Morris Water Maze Test

Three months after LG treatment, mice were subjected to a Morris water maze test in a round stainless steel pool (150 cm in diameter) filled with water (23 ± 1 °C) (Liang et al. 2004; Morris et al. 1982). After 24 h adaptation, mice were allowed to adapt to the maze for 120 s of free swimming. The mice were then trained in space learning tasks, and experiments were performed 4 times a day for 5 consecutive days. In the 24 h after the last training test, a 120-s probe test was performed in the absence of a hidden platform and their swimming path was recorded.

ELISA Assay

According to the ELISA kit, the protein concentration is screened first to calculate the amount of protein that the kit can react to. The standard protein and the sample protein were added to the well plates of the kit separately according to the group. At the same time, blank control wells were set up and kept overnight at 4 °C. The next day, washed the well plate 7 times with a special washing solution (both need to be properly plated for cleaning), added the labeled antibody (except for the blank control) and incubated at 37 °C for 1 h, added the coloring solution, and incubated at room temperature for 30 min. The OD value was measured with microplate reader (450 nm).

Statistical Analysis

All data are presented as the mean ± SEM, analyzed with one-way ANOVA followed by post hoc Turkey's tests where appropriate with drug treatment as the between-subjects factor. The significance level was set at $p < 0.05$.

Results

Effects of LG on Inflammation in Aβ-Treated N2A Cells

To examine the effect of LG on cell survival, we treated N2A cells with LG at different concentrations from 0 to 100 μM and then determined cell viability by the MTT assay. The results showed that LG had no effect on cell viability at all different concentrations (2.5 μM, 99.09 ± 1.97% relative to 0 μM, $p > 0.05$ vs. 0 μM; 5 μM, 96.23 ± 2.08% relative to 0 μM, $p > 0.05$ vs. 0 μM; 10 μM, 94.88 ± 4.81% relative to 0 μM, $p > 0.05$ vs. 0 μM; 20 μM, 93.71 ± 5.39% relative to 0 μM, $p > 0.05$ vs. 0 μM; 50 μM, 101.66 ± 5.78% relative to 0 μM, $p > 0.05$ vs. 0 μM; 100 μM, 94.27 ± 10.66% relative to 0 μM, $p > 0.05$ vs. 0 μM; Fig. 1a). Then, the N2A cells were treated with increasing concentrations of Aβ for 24 h to detect the cell viability that Aβ-induced. The results showed that Aβ treatment at the concentration of 10 μM or higher induced the death of N2A cells (2.5 μM, 91.72 ± 1.98% relative to 0 μM, $p > 0.05$ vs. 0 μM; 5 μM, 86.23 ± 2.09% relative to 0 μM, $p > 0.05$ vs. 0 μM; 10 μM, 74.08 ± 4.81% relative to 0 μM, $p < 0.05$ vs. 0 μM; 20 μM, 74.37 ± 5.39% relative to 0 μM, $p < 0.05$ vs. 0 μM; 50 μM, 64.66 ± 5.79% relative to 0 μM, $p < 0.01$ vs. 0 μM; 100 μM, 49.67 ± 10.25% relative to 0 μM, $p < 0.01$ vs. 0 μM; Fig. 1b). We next further investigated the effect of LG on Aβ-induced cell viability. After the pretreatment of Aβ (10 μM) for 4 h, N2A cells were treated with LG (0-200 μM) for 20 h in the presence of Aβ. The results showed that treatment with 20 μM LG rescued the cell viability that Aβ-induced (Aβ + 1 μM, 70.56 ± 4.32% relative to 0 μM, $p > 0.05$ vs. 0 μM; Aβ + 5 μM, 77.91 ± 5.72% relative to 0 μM, $p > 0.05$ vs. 0 μM; Aβ + 10 μM, 82.48 ± 7.95% relative to 0 μM, $p > 0.05$ vs. 0 μM; Aβ + 20 μM, 91.01 ± 12.2% relative to 0 μM, $p < 0.05$ vs. 0 μM; Aβ + 50 μM, 105.25 ± 10.12% relative to 0 μM, $p < 0.05$ vs. 0 μM; Aβ + 100 μM, 113.97 ± 9.52% relative to 0 μM, $p < 0.05$ vs. 0 μM; Aβ + 200 μM, 122.01 ± 13.02% relative to 0 μM, $p < 0.05$ vs. 0 μM; Fig. 1c). These results indicate that LG exhibits a protective role against Aβ-induced cell viability.

To future investigate the effect of LG treatment on the inflammation that Aβ-induced, we detected the expression of NLRP3 and caspase-1. The results showed that Aβ treatment dramatically increased the expression of NLRP3 (Aβ, 124.40 ± 4.03% relative to N2A, $p < 0.01$ vs. N2A; Fig. 1 d and g) and cleaved caspase-1 (Aβ, 190.84 ± 15.79% relative to N2A, $p < 0.01$ vs. N2A; Fig. 1 d and i) and LG treatment restored the Aβ-induced the increase of NLRP3 (Aβ + LG, 90.77 ± 8.48% relative to N2A, $p < 0.01$ vs. Aβ; Fig. 1 d and g) and cleaved caspase-1 (Aβ + LG, 126.18 ± 23.18%, $p < 0.01$ vs. N2A, $p < 0.01$ vs. Aβ; Fig. 1 d and i). Caspase-1 could induce the increase of caspase-3, leading to the apoptosis of the mitochondrial pathway (Hou et al. 2019). Then, we found that the treatment of LG inhibited the upregulation
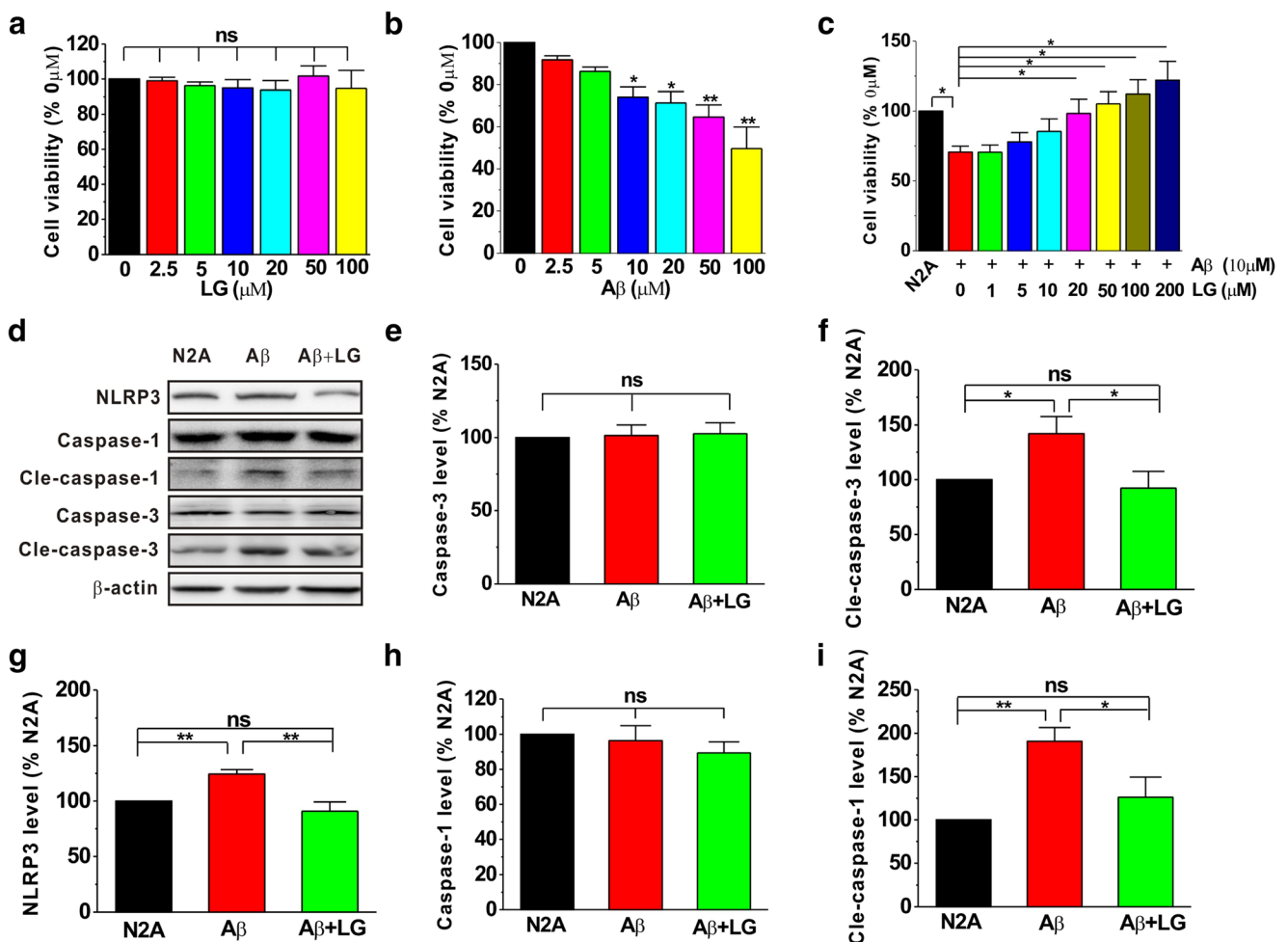
Fig. 1 LG reduces inflammation in Aβ-treated N2A cells. **a** LG treatment had no effect on cell viability in N2A cells ($n = 3$; one-way ANOVA: $F_{(6,14)} = 0.171$, $p = 0.98$). The cell viability is normalized by non-treatment with LG (0 μM). **b** Aβ reduced cell viability in N2A cells ($n = 3$; one-way ANOVA: $F_{(6,14)} = 10.380$, $p < 0.01$). **c** LG increased cell viability in a dose-dependent manner in Aβ-treated N2A cells ($n = 3$; one-way ANOVA: $F_{(6,14)} = 9.556$, $p < 0.01$). **d–i** Effects of LG on inflammation and apoptosis in Aβ-treated N2A cells. The relative protein levels of caspase-3 (**d** and **e**), cleaved caspase-3 (**d** and **f**), NLRP3 (**d** and **g**), caspase-1 (**d** and **h**), and cleaved caspase-1 (**d** and **i**) are normalized by N2A cells treated with Aβ ($n = 4$ in each group). One-way ANOVA: $F_{(2,9)} = 10.271$, $p = 0.03$ for NLRP3; $F_{(2,9)} = 0.048$, $p = 0.953$ for caspase-1; $F_{(2,9)} = 8.337$, $p = 0.009$ for cleaved caspase-1. Data are expressed as mean ± SEM, $*p < 0.05$, $**p < 0.01$

of cleaved caspase-3 (Aβ, 141.95 ± 15.58% relative to N2A, $p < 0.05$ vs. N2A; Aβ + LG, 92.23 ± 15.32% relative to N2A, $p > 0.05$ vs. N2A, $p < 0.05$ vs. Aβ; Fig. 1 d and f).

Effects of LG on Inflammation in Aβ-Treated BV2 Cells

To investigate the effect of LG treatment on the inflammation that Aβ-induced in the BV2 cells, we detected the expression of NLRP3 and caspase-1. The results showed that Aβ treatment dramatically increased the expression of NLRP3 (Aβ, 263.62 ± 31.39% relative to BV2, $p < 0.01$ vs. BV2; Fig. 2 a and b) and cleaved caspase-1 (Aβ, 196.57 ± 23.08% relative to BV2, $p < 0.01$ vs. BV2; Fig. 2 a and d) and LG treatment restored increase of NLRP3 that Aβ-induced (Aβ + LG, 107.22 ± 17.83% relative to BV2, $p > 0.05$ vs. BV2, $p < 0.01$ vs. Aβ; Fig. 2 a and b) and cleaved caspase-1 (Aβ + LG,

132.61 ± 15.24% relative to BV2, $p > 0.05$ vs. BV2, $p < 0.05$ vs. Aβ; Fig. 2 a and d). To further test the effect of LG treatment on the Th1 and Th2, Q-PCR was used to detected the mRNA level of IL-1β, TNF-α, IL-4, and IL-13. The results showed that Aβ significantly increased IL-1β (Aβ, 171.16 ± 9.02% relative to BV2, $p < 0.01$ vs. BV2; Fig. 2e) and TNF-α (Aβ, 167.38 ± 14.92% relative to BV2, $p < 0.01$ vs. BV2; Fig. 2f) mRNA levels and decreased IL-4 (Aβ, 64.48 ± 14.57%, $p < 0.05$ vs. BV2; Fig. 2g) and IL-13 (Aβ, 59.69 ± 8.77% relative to BV2, $p < 0.01$ vs. BV2; Fig. 2h) mRNA levels. LG treatment reduced the IL-1β (Aβ + LG, 113.08 ± 6.11% relative to BV2, $p > 0.05$ vs. BV2, $p < 0.01$ vs. Aβ; Fig. 2e) and TNF-α (Aβ + LG, 50.05 ± 7.89% relative to BV2, $p < 0.01$ vs. BV2, $p < 0.001$ vs. Aβ; Fig. 2f) and increased IL-4 (Aβ + LG, 159.01 ± 17.17%, $p < 0.01$ vs. BV2, $p < 0.05$ vs. BV2, $p < 0.001$ vs. Aβ; Fig. 2g) and IL-13 (Aβ
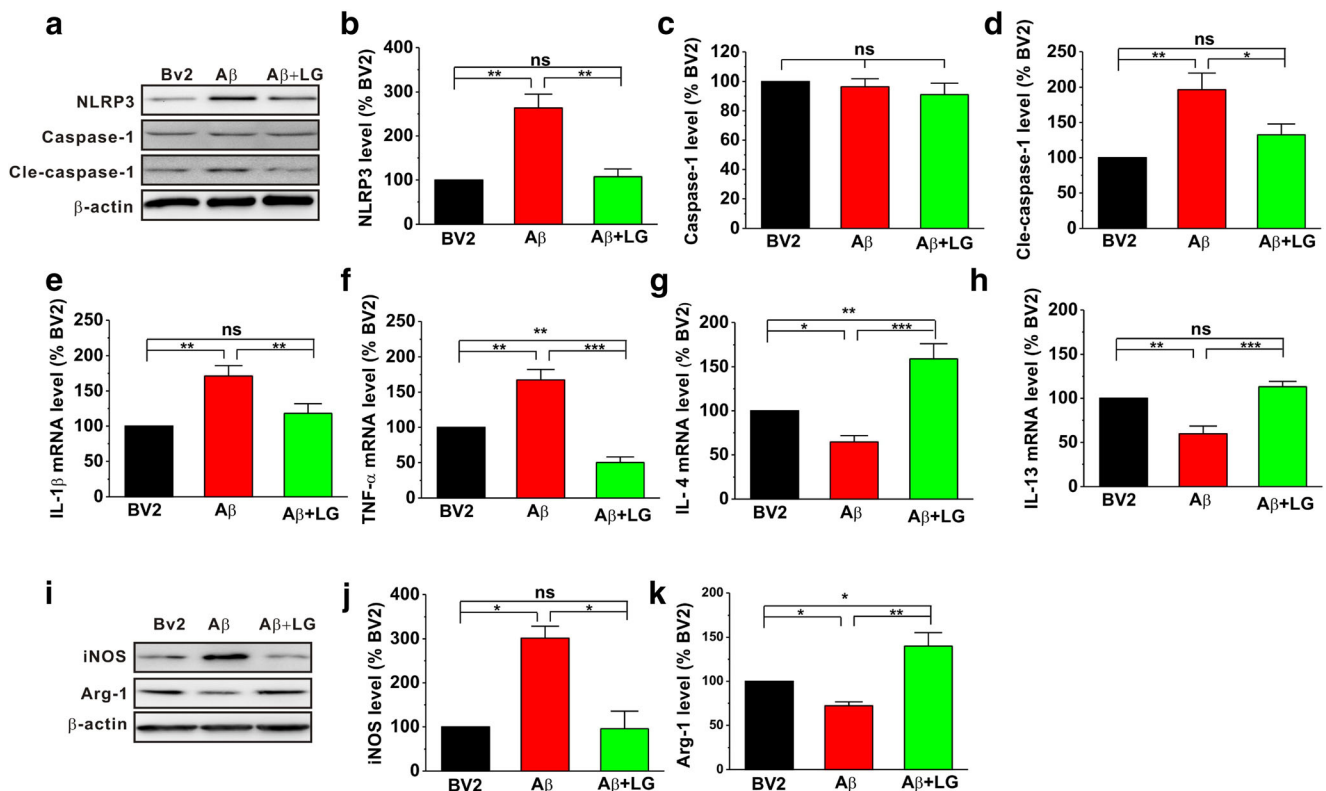
Fig. 2 LG reduces inflammation in Aβ-treated BV2 cells. The relative protein levels of NLRP3 (**a** and **b**), caspase-1 (**a** and **c**), and cleaved caspase-1 (**a** and **d**) are normalized by BV2 cells (*n* = 4 in each group). One-way ANOVA: $F_{(2,9)}$ = 16.679, *p* = 0.02 for NLRP3; $F_{(2,9)}$ = 0.669, *p* = 0.527 for caspase-1; $F_{(2,9)}$ = 9.466, *p* = 0.003 for cleaved caspase-1.

e–**h** IL-1β, TNF-α, Il-4, and IL-13 mRNA were determined by real-time. The relative protein levels of iNOS (**i** and **j**) and Arg-1 (**i** and **k**) are normalized by BV2 cells. Data are expressed as mean ± SEM, *p < 0.05, **p < 0.01

+ LG, 113.08 ± 6.11% relative to BV2, *p* > 0.05 vs. BV2, *p* < 0.001 vs. Aβ; Fig. 2h) mRNA to control level.

To investigate the effect of LG treatment on phenotypic transformation in BV2 cells that Aβ-induced, we detected the expression of M1 (iNOS) and M2 (Arg-1). The results showed that LG treatment decreased the expression of M1 (Aβ, 301.59 ± 27.01% relative to BV2, *p* < 0.05 vs. BV2; Aβ + LG, 95.56 ± 40.08% relative to BV2, *p* > 0.05 vs. BV2, *p* < 0.05 vs. Aβ; Fig. 2 i and j) and increased the expression of M2 (Aβ, 72.13 ± 4.36% relative to BV2, *p* < 0.05 vs. BV2; Aβ + LG, 139.93 ± 15.32% relative to BV2, *p* < 0.05 vs. N2A, *p* < 0.01 vs. Aβ; Fig. 2 i and k).

## Effects of LG on Learning and Memory in AD Mice

To evaluate the effects of LG on learning and memory in AD mice, the Morris water maze task was used. The results showed that the escape latency in the AD group was much longer than WT group (day 1, 71.31 ± 6.34 s for WT, 101.82 ± 3.27 s for AD; day 2, 37.24 ± 4.29 s for WT, 98.39 ± 7.16 s for AD; day 3, 27.34 ± 3.46 s for WT, 82.56 ± 5.66 s for AD; day 4, 21.31 ± 3.43 s for WT, 54.45 ± 8.14 s for AD; day 5, 17.94 ± 1.77 s for WT, 48.92 ± 9.13 s for AD; *p* < 0.01 vs. WT; Fig. 3a). LG treatment significantly shortened escape

latency for searching for the hidden platform (AD + LG, 97.4 ± 4.08 s for day 1; 67.29 ± 10.11 s for day 2; 34.52 ± 3.95 s for day 3; 29.82 ± 3.26 s for day 4; 17.34 ± 2.77 s for day 5; *p* < 0.01 vs. AD, *p* > 0.05 vs. WT; Fig. 3a), compared with those in the AD group. The probe test revealed that mice in AD group spent much less time in the target quadrant (WT, 40.22 ± 2.86 s; AD, 27.62 ± 2.18 s, *p* < 0.05 vs. WT; Fig. 3b) and reduced the number of entries into the platform zone (WT, 12.1 ± 0.78; AD, 7.5 ± 0.68, *p* < 0.05 vs. WT; Fig. 3c). LG treatment significantly increased the time spent in target quadrant (AD + LG, 46.51 ± 4.59 s, *p* > 0.05 vs. WT, *p* < 0.05 vs.AD; Fig. 3b) and the number of entries into the platform zone (AD + LG, 12.46 ± 1.56, *p* > 0.05 vs. WT, *p* < 0.05 vs. AD; Fig. 3c). Taken together, these results indicate that LG significantly ameliorates the memory deficits in AD mice.

Effects of LG on Inflammation and Apoptosis in the Brains of AD Mice

It has been well documented that NLRP3 and cleaved caspase-1 were the central role of the inflammation (Hou et al. 2019). The western blot was used to detect the expression of NLRP3 and cleaved caspase-1 in AD mice. The results showed that the expression of NLRP3 (AD, 151.10 ± 13.01%

Fig. 3 Effects of LG on spatial learning and memory of AD mice. **a** The escape latency to the hidden platform during spatial learning during the Morris water maze test. Repeated measures ANOVA: $F_{(2,12)} = 29.76$, $p < 0.01$. **b** During the probe test with absence of the hidden platform, the time spent in the hidden platform-located quadrant. One-way ANOVA: $F_{(2,12)} = 13.79$, $p < 0.01$. **c** The number of entries into the platform zone. One-way ANOVA: $F_{(2,12)} = 14.76$, $p < 0.01$. Data are expressed as mean ± SEM, $*p < 0.05$, $**p < 0.01$
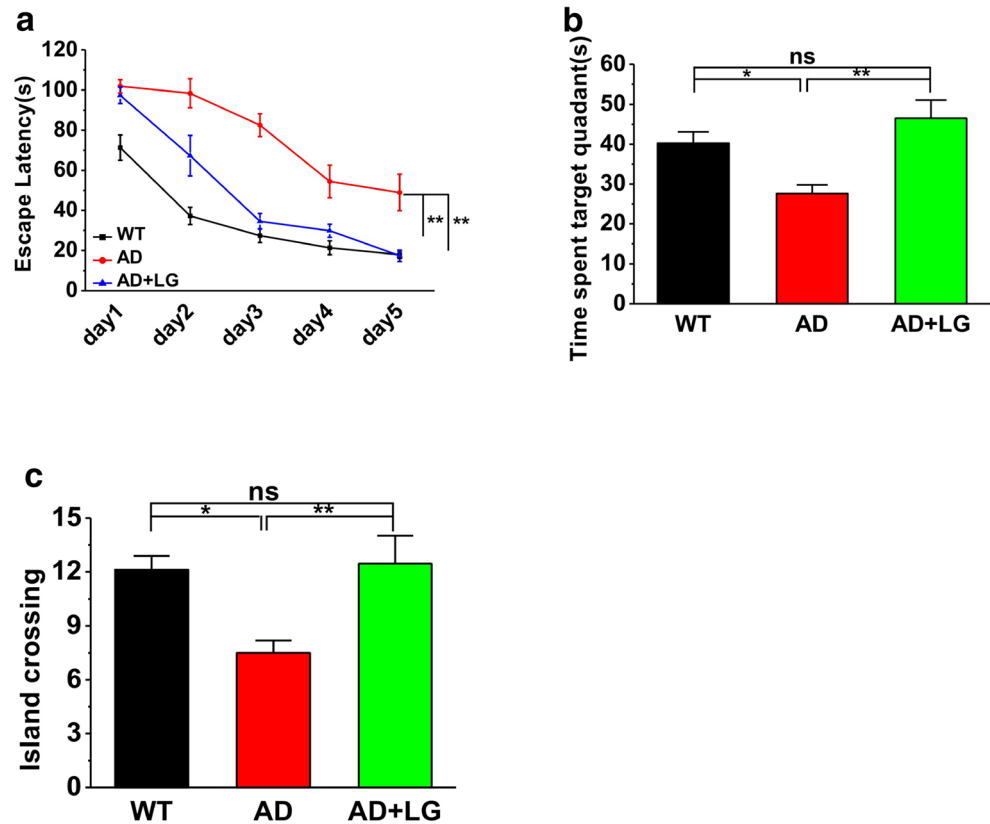
relative to WT, $p < 0.05$ vs. WT; Fig. 4a and B) and cleaved caspase-1 (AD, $212.12 \pm 18.09\%$ relative to WT, $p < 0.01$ vs. WT; Fig. 4 a and d) was increased in 6-month AD mice and LG treatment decreased the NLRP3 (AD + LG, $98.09 \pm 28.10\%$ relative to WT, $p > 0.05$ vs. WT; $p < 0.05$ vs. AD; Fig. 4 a and b) and cleaved caspase-1 expression (AD + LG, $148.10 \pm 16.08\%$ relative to WT, $p > 0.05$ vs. WT; $p < 0.05$ vs. AD; Fig. 4 a and d). To further test the effect of LG treatment on inflammatory cytokines, Q-PCR was used to detect the mRNA level of IL-1β and TNF-α. The results showed that Aβ significantly increased IL-1β (AD, $173.99 \pm 5.08\%$ relative to WT, $p < 0.001$ vs. WT; Fig. 4e) and TNF-α (AD, $206.69 \pm 33.05\%$ relative to WT, $p < 0.01$ vs. WT; Fig. 4f) mRNA levels. LG treatment restored the IL-1β (AD + LG, $59.77 \pm 11.27\%$ relative to WT, $p < 0.01$ vs. WT, $p < 0.01$ vs. AD; Fig. 4e) and TNF-α (AD + LG, 87.79 ± 5.33, $p > 0.05$ vs. WT, $p < 0.01$ vs. AD; Fig. 4f) mRNA levels. The data confirms that LG has an anti-inflammatory effect in AD mice.

Then, we examined the apoptosis-associated proteins caspase-3, BAX, and Bcl-2 in the brains of AD mice. We found that the treatment of LG decreased the expression of cleaved caspase-3 (AD, $312 \pm 18.01\%$ relative to WT, $p < 0.01$ vs. WT; AD + LG, $90.01 \pm 16.02\%$ relative to WT, $p > 0.05$ vs. WT, $p < 0.05$ vs. AD; Fig. 4 g and i) and BAX (AD, $138 \pm 17.01\%$ relative to WT, $p < 0.05$ vs. WT; AD + LG, $93.01 \pm 6.02\%$ relative to WT, $p > 0.05$ vs. WT, $p < 0.05$ vs. AD; Fig. 4 g and j) and increased the expression of Bcl-2 (AD, $33.01 \pm$

3.01% relative to WT, $p < 0.01$ vs. WT; AD + LG, $63.01 \pm 11.01\%$ relative to WT, $p < 0.05$ vs. WT, $p < 0.01$ vs. AD; Fig. 4 g and k). The results suggest that LG has an anti-apoptosis effect in AD mice.

Effects of LG on APP Processing in AD Mice

We found that LG significantly decreased the number of senile plaques (WT, $n = 10$ slices from 5 mice; AD, $n = 21$ slices from 7 mice, 76.86 ± 6.72, $p < 0.001$ vs. WT; AD + LG, $n = 21$ slices from 3 mice, 50.43 ± 4.83, $p < 0.001$ vs. WT; $p < 0.01$ vs. AD; Fig. 5 a and b). It is well known that senile plaques were consisted of Aβ deposition. However, Aβ is generated from sequential cleavages of APP by BACE1 and PS1 and BACE1 cleaves APP to generate C99 and C89 fragments, respectively (Hung and Livesey, 2018). Therefore, we detected whether LG can decrease the Aβ production. The results showed that LG decreased BACE1 (AD, $191 \pm 19\%$ relative to WT, $p < 0.01$ vs. WT; AD + LG, $99 \pm 12\%$ relative to WT, $p > 0.05$ vs. WT; $p < 0.01$ vs. AD; Fig. 5 c and e), C89 (AD, $190 \pm 19\%$ relative to WT, $p < 0.01$ vs. WT; AD + LG, $110 \pm 8\%$ relative to WT, $p > 0.05$ vs. WT; $p < 0.01$ vs.AD; Fig. 5 c and g), C99 (AD, $290 \pm 18\%$ relative to WT, $p < 0.01$ vs. WT; AD + LG, $120 \pm 12\%$ relative to WT, $p > 0.05$ vs. WT; $p < 0.01$ vs. AD; Fig. 5 c and h), PS1 (AD, $357 \pm 23\%$ relative to WT, $p < 0.01$ vs. WT; AD + LG, $64 \pm 8\%$ relative to WT, $p > 0.05$ vs. WT; $p < 0.01$ vs. AD; Fig. 5 c and f),
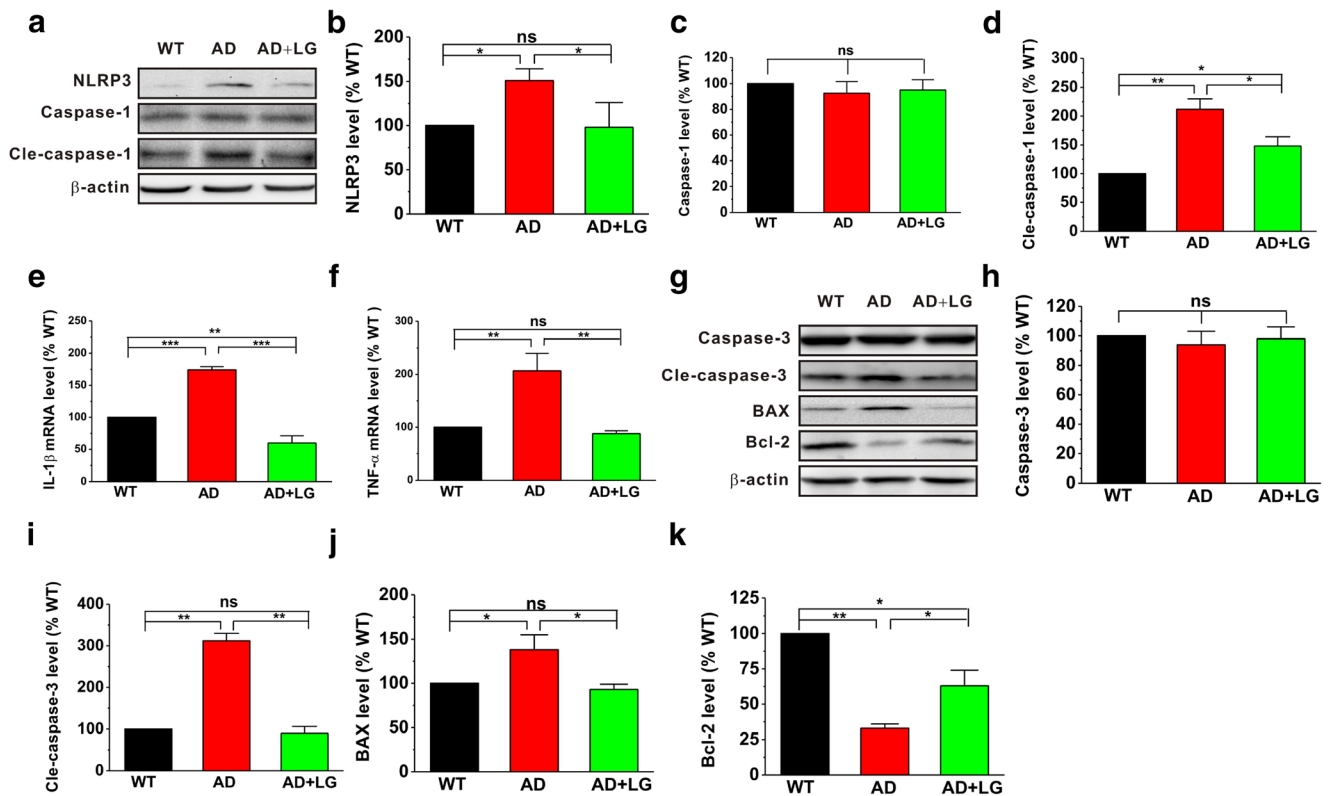
Fig. 4 Effects of LG on inflammation and apoptosis in AD mice. The relative protein levels of NLRP3 (a and b), caspase-1 (a and c), and cleaved caspase-1 (a and d) are normalized by AD mice ($n = 3$ in each group). One-way ANOVA: $F_{(2,6)} = 29.818$, $p < 0.01$ for NLRP3; $F_{(2,6)} = 3.378$, $p = 0.104$ for caspase-1; $F_{(2,6)} = 15.401$, $p < 0.01$ for cleaved cas-pase-1. IL-1β (e) and TNF-α (f) mRNA expressions were determined by real-time PCR. $n = 3–5$ in each group. Data are expressed as mean ± SEM, $*p < 0.05$, $**p < 0.01$. Effects of LG on apoptosis related proteins in AD mice. The relative protein levels of caspase-3 (g and h), cleaved caspase-3 (g and i), BAX (g and j), and Bcl-2 (g and k) are normalized by WT mice ($n = 3$ in each group)

Aβ42 (AD, 674.80 ± 34.97 relative to WT, $p < 0.001$ vs. WT; AD + LG, 583.54 ± 32.0466527.49 relative to WT, $p < 0.01$ vs. WT; $p < 0.01$ vs. AD; Fig. 5i), and Aβ40 (AD, 391.49 ± 60.03 relative to WT, $p < 0.01$ vs. WT; AD + LG, 251.27 ± 32.05 relative to WT, $p > 0.05$ vs. WT; $p < 0.05$ vs. AD; Fig. 5j) expression. However, the expression of APP was not af-fected by LG treatment (AD, 294.33 ± 28.01% relative to WT, $p < 0.01$ vs. WT; AD + LG, 307 ± 24.02% relative to WT, $p < 0.01$ vs. WT; $p > 0.05$ vs. AD; Fig. 5 c and d). Taken together, these results reveal that Aβ level is substantially reduced in AD mice treated with LG.

Effects of LG on Microglia M1/M2 Transformation in AD Mice

Two proteases, neprilysin (NEP) and insulin-degrading en-zyme (IDE), are generated from the microglial. To detect whether LG can affect the degradation of Aβ, western blot was used to study the expression of NEP and IDE. We found that LG treatment increased NEP (AD, 71.41 ± 3.92% relative to WT, $p < 0.05$ vs. WT; AD + LG, 127.26 ± 13.76% relative to WT, $p < 0.05$ vs. WT; $p < 0.05$ vs. AD; Fig. 6 a and b) and IDE (AD, 59.32 ± 12.99% relative to WT, $p < 0.05$ vs. WT;

AD + LG, 102.48 ± 12.41% relative to WT, $p > 0.05$ vs. WT; $p < 0.05$ vs. AD; Fig. 6 a and c) expressions. To future inves-tigate the effect of LG treatment on microglia M1/M2 trans-formation in AD mice, we detected the expression of Iba-1, M1 (iNOS), and M2 (Arg-1). The results showed that LG treatment decreased the expression of Iba-1 (AD, 158.49 ± 17.49% relative to WT, $p < 0.05$ vs. WT; AD + LG, 116.12 ± 14.07% relative to WT, $p > 0.05$ vs. WT, $p < 0.05$ vs. AD; Fig. 6 d and e) and M1 (AD, 158.04 ± 22.15% relative to WT, $p < 0.05$ vs. WT; AD + LG, 103.31 ± 19.51% relative to WT, $p > 0.05$ vs. WT, $p < 0.05$ vs. AD; Fig. 6 d and f); meanwhile, it increased the expression of M2 (AD, 73.71 ± 4.21% relative to WT, $p < 0.05$ vs. WT; AD + LG, 111.91 ± 13.28% relative to WT, $p < 0.05$ vs. WT, $p < 0.01$ vs. AD; Fig. 6 d and g).

Discussion

In the present study, we find that LG significantly reduced the Aβ-induced neuronal death and inflammatory response in N2A and BV2 cells. We also report that LG alleviates Aβ levels via decreasing Aβ generation, which may subsequently contribute to the amelioration of cognitive decline.
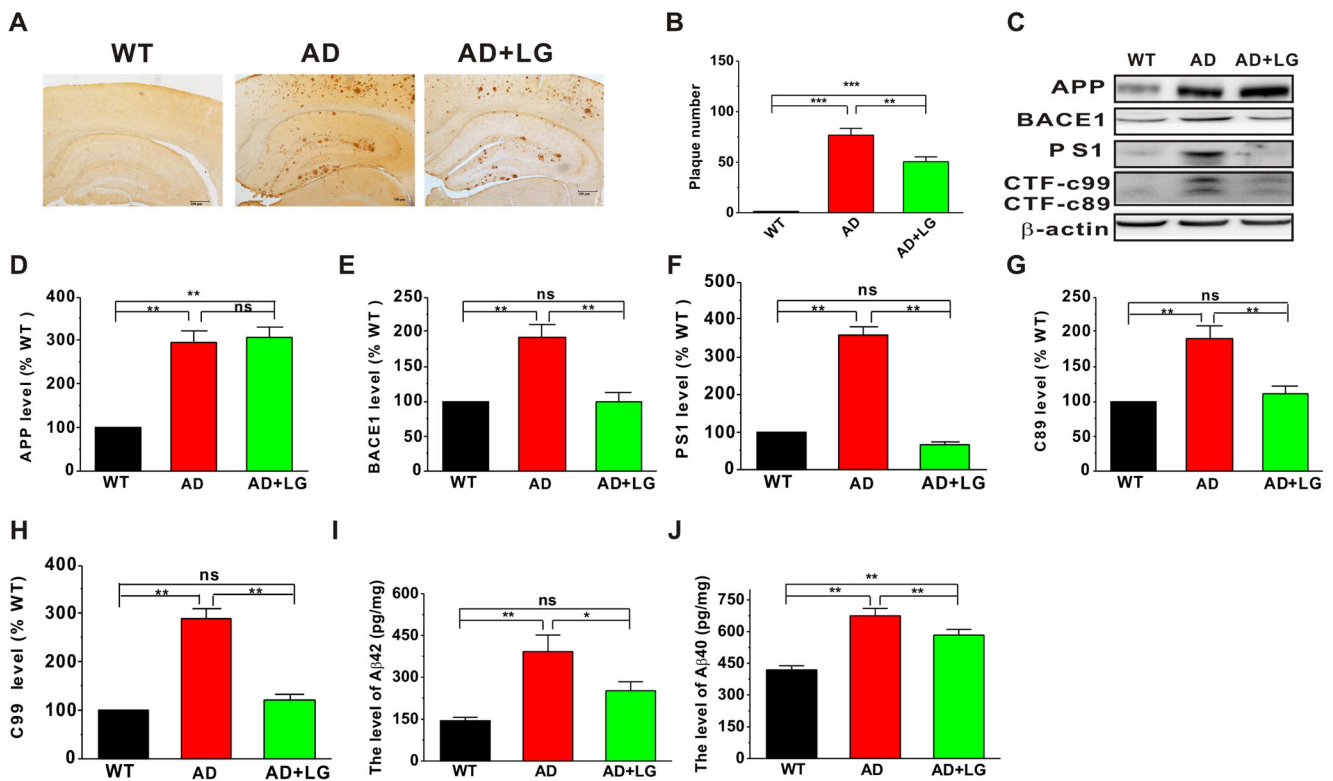
Fig. 5 LG decreases Aβ deposition in APP/PS1 mice. **a, b** The number of senile plaques were detected by immunohistochemistry in the brains of APP/PS1 mice with LG treatment ($n = 3$ in each group). One-way ANOVA: $F_{(2,12)} = 3.391$, $p = 0.144$. **c–h** Effects of LG on APP processing in AD mice. The relative protein levels of APP (**c** and **d**), BACE1 (**c** and **e**), PS1 (**c** and **f**), C88 (**c** and **g**), and C89 (**c** and **f**) are normalized by WT ($n = 5$ in each group). One-way ANOVA: $F_{(2,12)} = 25.773$, $p < 0.01$ for APP; $F_{(2,12)} = 14.831$, $p < 0.01$ for BACE1; $F_{(2,12)} = 79.349$, $p < 0.01$ for PS1; $F_{(2,12)} = 29.56$, $p < 0.01$ for C88; $F_{(2,12)} = 5.641$, $p < 0.05$ for PS1; $F_{(2,12)} = 42.2$, $p < 0.01$ for C89. **i, j** ELISA quantification of Aβ40 and Aβ42 was performed in APP/PS1 mice. Aβ40 levels and Aβ42 levels were markedly decreased after LG treatment. Data are expressed as mean ± SEM, *$p < 0.05$, **$p < 0.01$

Collectively, the current study demonstrates the LG's protective effect on the pathogenesis of AD, suggesting that LG may be a potential therapeutic agent for treating AD.

Alzheimer's disease (AD) is a progressive neurodegenerative disease characterized by extracellular deposition of Aβ-associated plaques (Li et al. 2018; van der Kant et al. 2019).
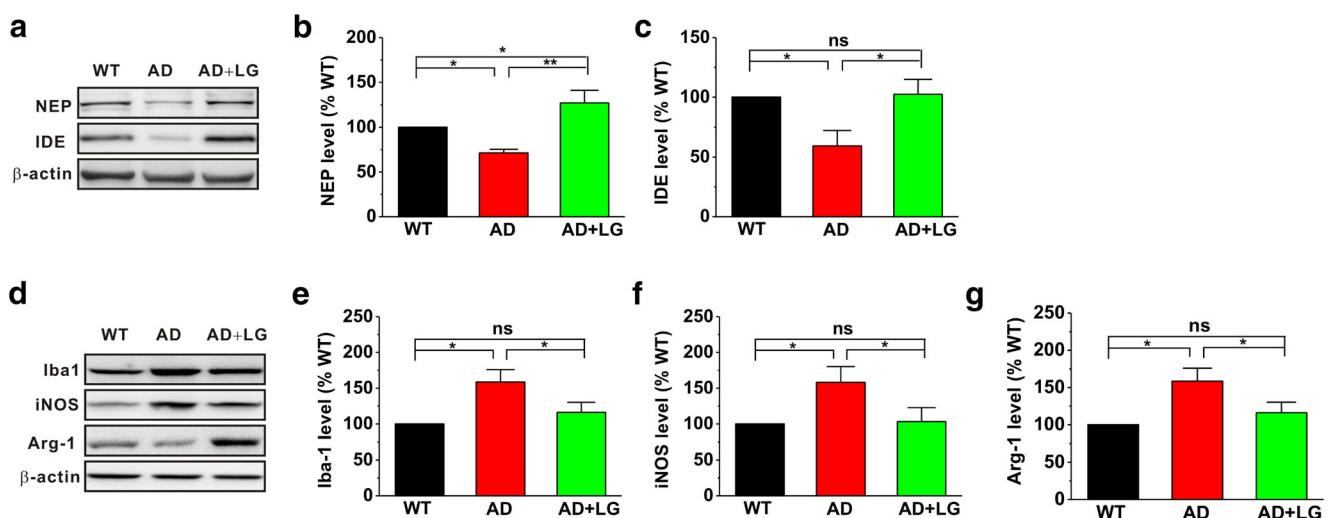

Fig. 6 Effects of LG on M1/M2 transformation in AD mice. The relative protein levels of NEP (**a** and **b**), IDE (**a** and **c**), Iba-1 (**d** and **e**), iNOS (**d** and **f**), and Arg-1 (**d** and **g**) are normalized by WT mice ($n = 4$ in each group). One-way ANOVA: $F_{(2,9)} = 3.657$, $p = 0.069$ for iNOS; $F_{(2,9)} = 5.910$, $p = 0.023$ for Arg-1; $F_{(2,9)} = 5.435$, $p = 0.014$ for Iba-1. Data are expressed as mean ± SEM, *$p < 0.05$, **$p < 0.01$

Aβ has been considered to be a key role in the pathogenesis of AD and the accumulation of Aβ induced tau hyperphosphorylation, inflammatory response, and neuronal apoptosis (Kunkle et al. 2019). Thus, reducing the amount of Aβ might be a potential therapeutic strategy for AD. It has been demonstrated that LG could alleviate the Aβ-induced neurotoxicity effects in the neuron cells (Jo et al. 2016b). Accordingly, in the present study, we found that LG could decrease the inflammatory reaction and neuronal apoptosis in N2A cells. Meanwhile, we found that Aβ treatment induced the increase of M1 type microglia and decrease of M2 type microglia in the BV2 cells, which could be reversed by LG.

Aβ is generated by the sequential action of proteases denoted as β-secretase (BACE1) and γ-secretase, which cleave the amyloid precursor protein (APP) (Kimura et al. 2016). In this study, we demonstrated that LG could decrease the expression of BACE1, PS1, and CTF, thereby reducing the Aβ production, but have no effect on APP expression in AD mice.

Neuroinflammation, by activating microglia, also plays a key role in the onset and development of AD (Li et al. 2019; Thawkar and Kaur, 2019). NLRP3 is the representative inflammasome, and previous studies have demonstrated that NLRP3 knockout mice decreased the deposition of Aβ, restored synaptic plasticity, and improved cognitive function (Tejera et al. 2019; Yin et al. 2018). Therefore, it is reasonable to speculate that LG could decrease the NLRP3 expression and thereby increasing the clearance of Aβ. There are two types of activated microglia: M1 and M2 (Allendorf et al. 2019). The activation of M1 microglia produces a range of inflammation factors, including IL-1β, IL-6, and TNF-α, and promotes the neuroinflammation (Gupta et al. 2018). NLRP3 is able to activate the pro-inflammatory protein caspase-1 and thus promote the secretion of IL-1β (Long et al. 2019). In our study, we found that LG could decrease the expression of cleaved caspase-1 and IL-1β as well as the TNF-α mRNA levels, while M2 microglia, such as IL-4 and IL-13, can release anti-inflammatory factors, phagocytosis of damaged nerve cell fragments, and promotion of tissue repair and neuron regeneration (Liu et al. 2019). In our study, we reported that LG could activate the M2 microglia, as reflected by the increase of Arg-1 expression. We also found that LG could rescue the expression IDE and NEP; therefore, it is reasonable to suggest that LG could regulate the microglia M1/M2 balance to accelerate the clearance of Aβ.

In addition, the present study showed that LG treatment ameliorated the learning and memory deficits in AD mice. Taken together, the results demonstrate that LG could decrease the Aβ production and accelerate the Aβ clearance by regulating the microglia M1/M2 transformation, thereby alleviating the cognitive impairments, suggesting a potential therapeutic role of LG for AD patients.

Compliance with Ethical Standards

References

Qiang W, Yau WM, Lu JX, Collinge J, Tycko R (2017) Structural variation in amyloid-beta fibrils from Alzheimer's disease clinical subtypes. Nature 541(7636):217–221

Nakamura A, Kaneko N, Villemagne VL, Kato T, Doecke J, Dore V, Fowler C, Li QX, Martins R, Rowe C et al (2018) High performance plasma amyloid-beta biomarkers for Alzheimer's disease. Nature 554(7691):249–254

Takasugi N, Tomita T, Hayashi I, Tsuruoka M, Niimura M, Takahashi Y, Thinakaran G, Iwatsubo T (2003) The role of presenilin cofactors in the gamma-secretase complex. Nature 422(6930):438–441

Bohm C, Chen F, Sevalle J, Qamar S, Dodd R, Li Y, Schmitt-Ulms G, Fraser PE, St George-Hyslop PH (2015) Current and future implications of basic and translational research on amyloid-beta peptide production and removal pathways. Mol Cell Neurosci 66(Pt A):3–11

Tan JZA, Gleeson PA (2019) The role of membrane trafficking in the processing of amyloid precursor protein and production of amyloid peptides in Alzheimer's disease. Biochim Biophys Acta Biomembr 1861(4):697–712

Jang JY, Rhim H, Kang S (2018) NABi, a novel beta-sheet breaker, inhibits Abeta aggregation and neuronal toxicity: therapeutic implications for Alzheimer's disease. Biochim Biophys Acta, Gen Subj 1862(1):71–80

Kong Y, Ruan L, Qian L, Liu X, Le Y (2010) Norepinephrine promotes microglia to uptake and degrade amyloid beta peptide through up-regulation of mouse formyl peptide receptor 2 and induction of insulin-degrading enzyme. J Neurosci 30(35):11848–11857

Gogoleva VS, Drutskaya MS, Atretkhany KS (2019) The role of microglia in the homeostasis of the central nervous system and neuroinflammation. Mol Biol 53(5):790–798

Hurtley SM (2017) A microglia type associated with AD. Science 357(6347):160–161

Liu FQ, Gao Q, Wang DD, Zhang ZX (2018) Effects of GBE50 on LPS/ATP induced NLRP3 inflammasome activation in primary rat microglia. Zhongguo Zhong yao za zhi = Zhongguo zhongyao zazhi. China J Chin Materia Medica 43(16):3346–3352

Garcez ML, Mina F, Bellettini-Santos T, da Luz AP, Schiavo GL, Macieski JMC, Medeiros EB, Marques AO, Magnus NQ, Budni J (2019) The involvement of NLRP3 on the effects of minocycline in

an AD-like pathology induced by beta-amyloid oligomers administered to mice. Mol Neurobiol 56(4):2606–2617

Chan EWL, Krishnansamy S, Wong C, Gan SY (2019) The NLRP3 inflammasome is involved in the neuroprotective mechanism of neural stem cells against microglia-mediated toxicity in SH-SY5Y cells via the attenuation of tau hyperphosphorylation and amyloidogenesis. Neurotoxicology 70:91–98

Fan Z, Liang Z, Yang H, Pan Y, Zheng Y, Wang X (2017) Tenuigenin protects dopaminergic neurons from inflammation via suppressing NLRP3 inflammasome activation in microglia. J Neuroinflammation 14(1):256

Sierra-Filardi E, Puig-Kroger A, Blanco FJ, Nieto C, Bragado R, Palomero MI, Bernabeu C, Vega MA, Corbi AL (2011) Activin A skews macrophage polarization by promoting a proinflammatory phenotype and inhibiting the acquisition of anti-inflammatory macrophage markers. Blood 117(19):5092–5101

Yousefi N, Sotoodehnejadnematalahi F, Heshmati-Fakhr N, Sayyah M, Hoseini M, Ghassemi S, Aliakbari S, Pourbadie HG (2019) Prestimulation of microglia through TLR4 pathway promotes interferon beta expression in a rat model of Alzheimer's disease. J Molec Neurosci 67(4):495–503

Ji J, Xue TF, Guo XD, Yang J, Guo RB, Wang J, Huang JY, Zhao XJ, Sun XL (2018) Antagonizing peroxisome proliferator-activated receptor gamma facilitates M1-to-M2 shift of microglia by enhancing autophagy via the LKB1-AMPK signaling pathway. Aging Cell 17(4):e12774

Zhu X, Shi J, Li H (2018) Liquiritigenin attenuates high glucose-induced mesangial matrix accumulation, oxidative stress, and inflammation by suppression of the NF-kappaB and NLRP3 inflammasome pathways. Biomed Pharmacotherap 106:976–982

Ramalingam M, Kim H, Lee Y, Lee YI (2018) Phytochemical and pharmacological role of liquiritigenin and isoliquiritigenin from Radix Glycyrrhizae in human health and disease models. Front Aging Neurosci 10:348

Jo DS, Shin DW, Park SJ, Bae JE, Kim JB, Park NY, Kim JS, Oh JS, Shin JW, Cho DH (2016a) Attenuation of Abeta toxicity by promotion of mitochondrial fusion in neuroblastoma cells by liquiritigenin. Arch Pharm Res 39(8):1137–1143

Hongyan L, Suling W, Weina Z, Yajie Z, Jie R (2016) Antihyperuricemic effect of liquiritigenin in potassium oxonate-induced hyperuricemic rats. Biomed Pharmacotherap 84:1930–1936

Liu RT, Zou LB, Lu QJ (2009) Liquiritigenin inhibits Abeta(25-35)-induced neurotoxicity and secretion of Abeta(1-40) in rat hippocampal neurons. Acta Pharmacol Sin 30(7):899–906

Theriault P, ElAli A, Rivest S (2016) High fat diet exacerbates Alzheimer's disease-related pathology in APPswe/PS1 mice. Oncotarget 7(42):67808–67827

Katoh R, Bray CE, Suzuki K, Komiyama A, Hemmi A, Kawaoi A, Oyama T, Sugai T, Sasou S (1995) Growth activity in hyperplastic and neoplastic human thyroid determined by an immunohistochemical staining procedure using monoclonal antibody MIB-1. Hum Pathol 26(2):139–146

Morris RG, Garrud P, Rawlins JN, O'Keefe J (1982) Place navigation impaired in rats with hippocampal lesions. Nature 297(5868):681–683

Liang H, Salinas RA, Leal BZ, Kosakowska-Cholody T, Michejda CJ, Waters SJ, Herman TS, Woynarowski JM, Woynarowska BA (2004) Caspase-mediated apoptosis and caspase-independent cell death induced by irofulven in prostate cancer cells. Mol Cancer Ther 3(11):1385–1396

Hou Z, Li F, Chen J, Liu Y, He C, Wang M, Mei T, Zhang Y, Song L, Shao X (2019) Beneficial effects of sagacious Confucius' pillow elixir on cognitive function in senescence-accelerated P8 mice (SAMP8) via the NLRP3/caspase-1 pathway. Evid-Based Complement Altern med: eCAM 2019:3097923

Hung COY, Livesey FJ (2018) Altered gamma-secretase processing of APP disrupts lysosome and autophagosome function in monogenic Alzheimer's disease. Cell Rep 25(13):3647–3660 e3642

Li S, Jin M, Liu L, Dang Y, Ostaszewski BL, Selkoe DJ (2018) Decoding the synaptic dysfunction of bioactive human AD brain soluble Abeta to inspire novel therapeutic avenues for Alzheimer's disease. Acta Neuropathologic Commu 6(1):121

van der Kant R, Goldstein LSB, Ossenkoppele R (2019) Amyloid-beta-independent regulators of tau pathology in Alzheimer disease. Nat Rev Neurosci

Kunkle BW, Grenier-Boley B, Sims R, Bis JC, Damotte V, Naj AC, Boland A, Vronskaya M, van der Lee SJ, Amlie-Wolf A et al (2019) Genetic meta-analysis of diagnosed Alzheimer's disease identifies new risk loci and implicates Abeta, tau, immunity and lipid processing. Nat Genet 51(3):414–430

Jo DS, Shin DW, Park SJ, Bae JE, Kim JB, Park NY, Kim JS, Oh JS, Shin JW, Cho DH (2016b) Erratum to: Attenuation of Abeta toxicity by promotion of mitochondrial fusion in neuroblastoma cells by liquiritigenin. Arch Pharm Res 39(9):1337

Kimura A, Hata S, Suzuki T (2016) Alternative selection of beta-site APP-cleaving enzyme (BACE1) cleavage sites in amyloid beta-protein precursor (APP) harboring protective and pathogenic mutations within the Abeta sequence. J Biol Chem 291(46):24041–24053

Thawkar BS, Kaur G (2019) Inhibitors of NF-kappaB and P2X7/NLRP3/Caspase 1 pathway in microglia: novel therapeutic opportunities in neuroinflammation induced early-stage Alzheimer's disease. J Neuroimmunol 326:62–74

Li Q, Liu D, Pan F, Ho CSH, Ho RCM (2019) Ethanol exposure induces microglia activation and neuroinflammation through TLR4 activation and SENP6 modulation in the adolescent rat hippocampus. Neural Plasticity 2019:1648736

Yin J, Zhao F, Chojnacki JE, Fulp J, Klein WL, Zhang S, Zhu X (2018) NLRP3 Inflammasome inhibitor ameliorates amyloid pathology in a mouse model of Alzheimer's disease. Mol Neurobiol 55(3):1977–1987

Tejera D, Mercan D, Sanchez-Caro JM, Hanan M, Greenberg D, Soreq H, Latz E, Golenbock D, Heneka MT (2019) Systemic inflammation impairs microglial Abeta clearance through NLRP3 inflammasome. EMBO J 38(17):e101064

Allendorf DH, Puigdellivol M, Brown GC (2019) Activated microglia desialylate their surface, stimulating complement receptor 3-mediated phagocytosis of neurons. Glia

Gupta N, Shyamasundar S, Patnala R, Karthikeyan A, Arumugam TV, Ling EA, Dheen ST (2018) Recent progress in therapeutic strategies for microglia-mediated neuroinflammation in neuropathologies. Expert Opin Ther Targets 22(9):765–781

Long J, Wang Q, He H, Sui X, Lin G, Wang S, Yang J, You P, Luo Y, Wang Y (2019) NLRP3 inflammasome activation is involved in trimethyltin-induced neuroinflammation. Brain Res 1718:186–193

Liu Y, Zeng R, Wang Y, Huang W, Hu B, Zhu G, Zhang R, Li F, Han J, Li Y (2019) Mesenchymal stem cells enhance microglia M2 polarization and attenuate neuroinflammation through TSG-6. Brain Res 1724:146422